



UNIVERSITÀ  
DEGLI STUDI  
FIRENZE

FLORE

## Repository istituzionale dell'Università degli Studi di Firenze

### **Alpine metamorphic and tectonic evolution of the Inzecca-Ghisoni area (Southern Alpine Corsica, France)**

Questa è la Versione finale referata (Post print/Accepted manuscript) della seguente pubblicazione:

*Original Citation:*

Alpine metamorphic and tectonic evolution of the Inzecca-Ghisoni area (Southern Alpine Corsica, France) / F. GARFAGNOLI; F. MENNA; E. PANDELI; G. PRINCIPI. - In: GEOLOGICAL JOURNAL. - ISSN 0072-1050. - STAMPA. - 44:(2009), pp. 1-20. [10.1002\GJ.1141]

*Availability:*

This version is available at: 2158/369135 since:

*Published version:*

DOI: 10.1002\GJ.1141

*Terms of use:*

Open Access

La pubblicazione è resa disponibile sotto le norme e i termini della licenza di deposito, secondo quanto stabilito dalla Policy per l'accesso aperto dell'Università degli Studi di Firenze (<https://www.sba.unifi.it/upload/policy-oa-2016-1.pdf>)

*Publisher copyright claim:*

(Article begins on next page)

## Alpine metamorphic and tectonic evolution of the Inzecca-Ghisoni area (southern Alpine Corsica, France)

FRANCESCA GARFAGNOLI<sup>1\*</sup>, FRANCESCO MENNA<sup>1</sup>,  
ENRICO PANDELI<sup>1,2</sup> and GIANFRANCO PRINCIPI<sup>1,2</sup>

<sup>1</sup>Department of Earth Sciences, University of Florence, Via G. La Pira, 4, 50121 Florence, Italy

<sup>2</sup>CNR-IGG, Section of Florence, Via G. La Pira, 4, 50121 Florence, Italy

---

In the Inzecca-Ghisoni area (southern Alpine Corsica), a complex assemblage of vertically juxtaposed tectonic units, affected by Alpine deformations and metamorphism, crops out. Among them, there are some tectonic units (Parautochthonous Units, i. e. *parautochtone* of previous studies), that represent fragments of the continental Corse basement (Palaeozoic granitoids and associated volcanic and metamorphic pre-Carboniferous rocks) and of its Mesozoic to Tertiary sedimentary cover, that are tectonically sliced between the allochthonous Ligurian-Piedmontese Units (Schistes Lustrés) and the autochthonous basement (Variscan Corsica). The reconstructed polyphase deformation and metamorphic evolution of such units and the finding of high-pressure/low-temperature mineral assemblages in the continental-derived tectonic slices, points to the involvement of the south-eastern border of the European basement of Corsica in the tectonic processes linked to the Alpine subduction. Copyright © 2009 John Wiley & Sons, Ltd.

Received 9 January 2008; accepted 28 October 2008

KEY WORDS Alpine Corsica; Inzecca; high-pressure/low-temperature metamorphism; continental-derived tectonic slices; deformative phases

### 1. INTRODUCTION

Many recent works carried out on the Alpine Corsica pointed out that Tertiary deformations associated to high-pressure/low-temperature (HP/LT) metamorphism occurred not only in the oceanic metamorphic units, that is Schistes Lustrés, as it has long been known (Lahondère and Guerrot 1997; Brunet *et al.* 2000 and references therein), but also in the tectonic slices derived from the continental margin of the European Plate (Amaudric du Chaffaut *et al.* 1976; Amaudric du Chaffaut and Saliot 1979; Bezert and Caby 1988, 1989; Tribuzio and Giacomini 2002; Molli and Tribuzio 2004; Malasoma *et al.* 2006; Molli *et al.* 2006).

In this paper we show the results of a geological study performed in the southernmost sector of the boundary between Alpine Corsica and Variscan Corsica (Figure 1). Through a new 1:10000 scale geological mapping (Figure 2), structural analyses at the meso- and micro-scale, and petrographical and mineral chemistry analyses, we provide new data that point out the occurrence of Alpine polyphase deformation and HP/LT metamorphism in the parautochthonous continental-derived units, stacked between the Schistes Lustrés of Alpine Corsica and the autochthonous basement. These data support the hypothesis of the involvement of the European margin (i.e. Corsica margin) in the subduction-related tectonics during the Alpine Orogeny. The deformation and metamorphic evolution of the studied area is also outlined.

\* Correspondence to: F. Garfagnoli, Department of Earth Sciences, University of Florence, Via La Pira, 4, 50121 Florence, Italy.  
E-mail: francesca.garfagnoli@geo.unifi.it

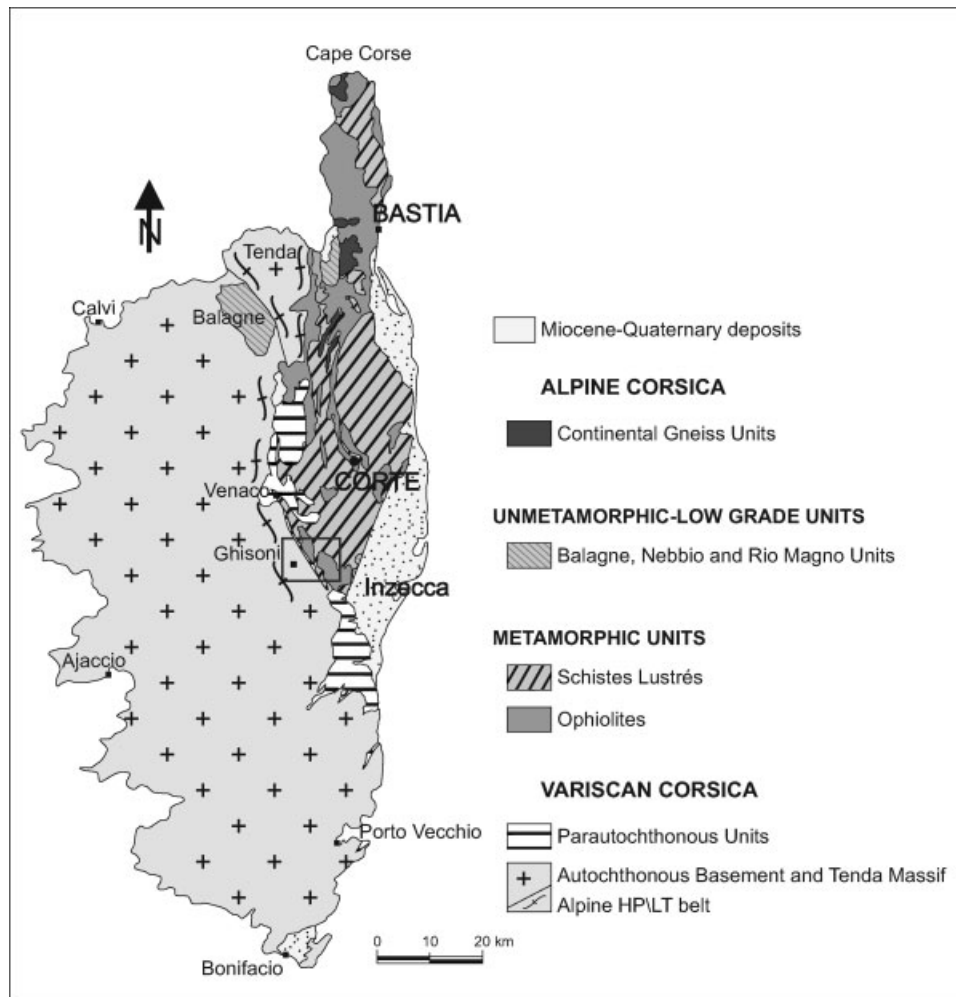


Figure 1. Geological sketch map of Corsica with location of the studied area in the box (redrawn after Durand-Delga 1984 and Zarki-Jakni *et al.* 2004).

## 2. GEOLOGICAL BACKGROUND

The island of Corsica is formed of two different geological domains (Figure 1): (a) Variscan Corsica, which represents the western two-thirds of the island and is made up of Carboniferous to Permian granitoids with associated volcanic and Lower Palaeozoic metamorphic country rocks (Menot and Orsini 1990; Cocherie *et al.* 2005; Elter and Pandeli 2005) and remnants of a Late-Palaeozoic–Late Eocene sedimentary cover (Durand-Delga 1984); (b) Alpine Corsica, which constitutes the remaining north-eastern part of the island and it is constituted by a complex tectonic pile including both metamorphic oceanic- (Schistes Lustrés) and continental-derived (e.g. Serra di Pigno/Farinole, Centuri) thrust sheets (Durand-Delga 1978, 1984). Non-metamorphic or very low grade, mainly ophiolitic units (*Nappes Supérieures*, e.g. the Ligurian Units of the Balagne, Macinaggio, Rio Magno Unit and Pineto Unit) also occur at the top of the tectonic stack (Marroni and Pandolfi 2003). The Schistes Lustrés are underlain by continental-derived tectonic units such as the Tenda Massif, the Corte slices, the Santa Lucia Unit and

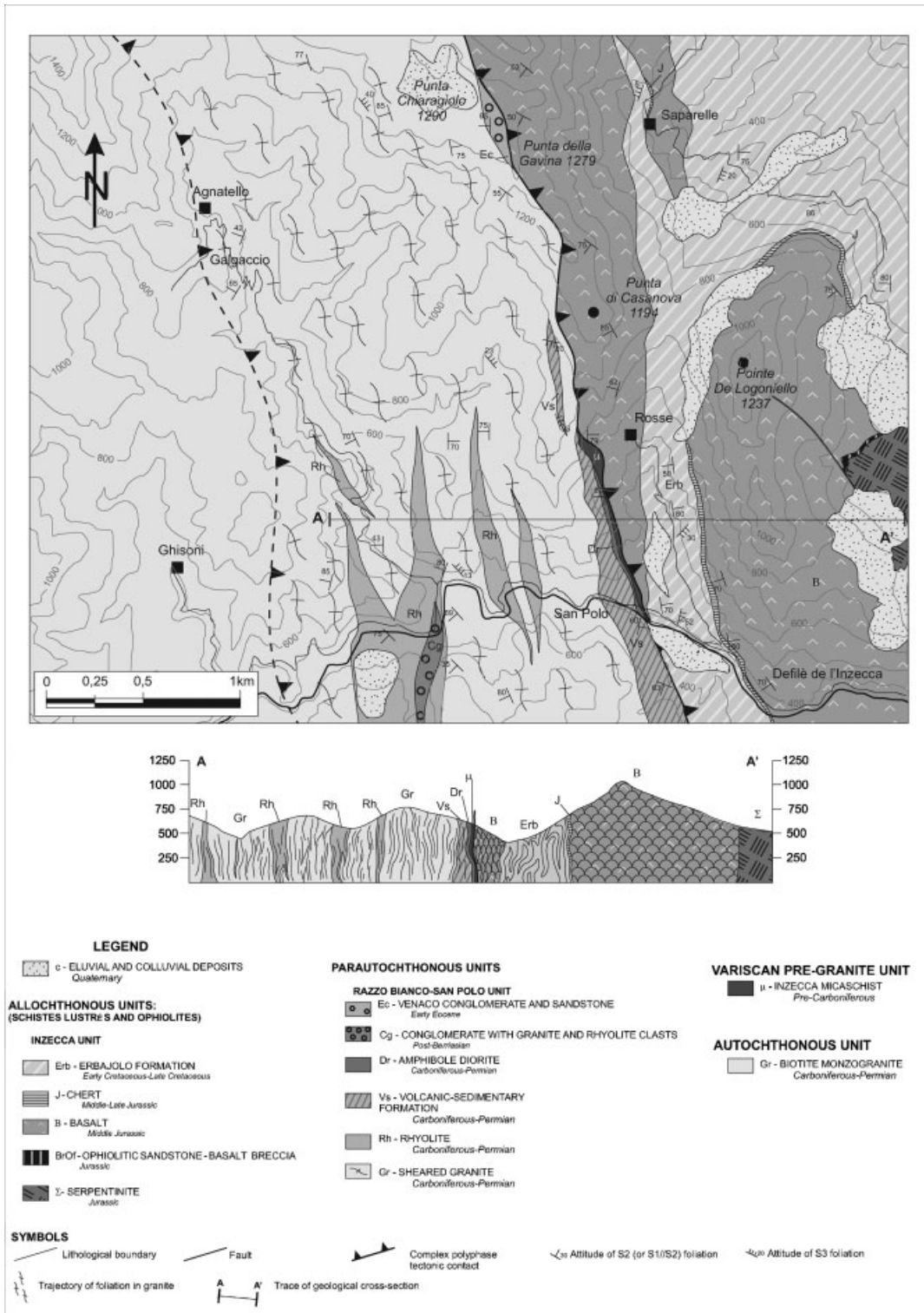


Figure 2. Geological schematic map of the studied area based on the 1:10 000 scale geological survey by the authors.

the Caporalino-Pedani Unit (Durand-Delga 1984 and references therein), that are considered to be Alpine tectonic slices of the European margin (Parautochthonous Units, i. e. *parautochtone* in Amaudric du Chaffaut *et al.* 1985a,b), including parts of the crystalline Palaeozoic basement and of its Late Carboniferous-Mesozoic to Middle Eocene sedimentary covers; they are characterized by an Alpine polyphase deformation and evolution, associated to metamorphism, ranging from HP/LT metamorphism, in the low-grade to epidote-blueschist facies, to greenschist facies conditions (Amaudric du Chaffaut *et al.* 1976; Amaudric du Chaffaut and Saliot 1979; Gibbons and Horak 1984; Bezert and Caby 1988; Molli and Tribuzio 2004; Malasoma *et al.* 2006).

The oceanic units derived from the Ligurian-Piedmontese domain (the Schistes Lustrés and the non-metamorphic Ligurian Units), developed between the European continent and Adria microplate, through Triassic rifting and Jurassic spreading phases (Bortolotti *et al.* 2001). During the Alpine Orogeny, these units experienced oceanic subduction, with the development of an accretionary wedge, and Late Cretaceous to Eocene HP/LT metamorphism, ranging from low-grade to blueschist facies up to eclogite facies (Maluski 1977; Mattauer *et al.* 1977; Harris 1985; Caron and Péquignot, 1986; Warburton 1986; Lahondère 1988; Egal 1992; Caron 1994; Lahondère and Guerrot 1997; Jolivet *et al.* 1998; Malavieille *et al.* 1998; Brunet *et al.* 2000). According to Malavieille *et al.* (1998), the following continent-continent (Europe versus Adria) collision determined the involvement of European continental slices in the subduction zone, as suggested by the HP/LT metamorphic imprint, recognized in the Parautochthonous Units. In particular: 'epidote-blueschist facies' (assemblage: riebeckite+celadonite-rich phengite+epidote+quartz) metamorphism (Tribuzio and Giacomini 2002; Molli and Tribuzio 2004; Molli *et al.* 2006) or 'low-blueschist facies' (assemblage: riebeckite+celadonite-rich phengite+quartz+albite+epidote) metamorphism (Malasoma *et al.* 2006 and references therein) were found in the parautochthonous rocks of the Tenda Massif and of more external areas (e.g. Popolasca-Francardo), respectively. The Alpine Corsica units were later exhumed during their westwards thrusting onto the Variscan Corsica (Durand-Delga 1978; Mattauer *et al.* 1981) or through low-angle ductile and brittle normal faulting according to the 'core complex' extensional model (Jolivet *et al.* 1990, 1991; Daniel *et al.* 1996).

During this stage, the HP/LT rocks were metamorphosed under decreasing pressure conditions reaching the greenschist facies (Daniel *et al.* 1996; Brunet *et al.* 2000 and references therein).

The previously thickened orogenic wedge collapsed during the Oligocene to Early Miocene time interval, because of the onset of large-scale extension (Brunet *et al.* 2000 and references therein).

During Early–Middle Miocene times, the opening of the Liguro-Provençal and Tyrrhenian basins isolated Alpine Corsica from the surrounding collisional belts (Faccenna *et al.* 1997; Jolivet *et al.* 1998; Speranza *et al.* 2002) and marine sediments deposited in the coeval St. Florent, Francardo and Aleria basins, sealing the tectonic contacts between the stacked units (Dallan and Puccinelli 1995; Ferrandini *et al.* 1998; Fellin *et al.* 2005 and references therein). Since Tortonian times, strike-slip or normal faulting and large-scale folding (e.g. the N–S-trending Castigniccia-Cape Corse mega-antiform) finally deformed both the tectonic stack and the overlying Miocene sedimentary basins (Faure and Malavieille 1981; Amaudric du Chaffaut 1982; Durand-Delga 1978, 1984; Fellin *et al.* 2005; Cavazza *et al.* 2007).

### 3. GEOLOGY OF THE INZECCA-GHISONI AREA

#### 3.1. Geological setting

The study area is located at the southern tip of the Alpine Corsica, between the Inzecca Massif to the east and the village of Ghisoni to the west (Figure 1), along the course of the Fium'Orbo River, which cuts through almost orthogonally the tectonic contacts between the Schistes Lustrés, the Parautochthonous Units and the Autochthonous Units (i.e. the contact between Alpine and Variscan Corsica).

The tectonic pile shows an overall vertical attitude and a N–S-trending strike. The following stratigraphic partitions have been distinguished within each of the tectonic units (from the base of the pile) (Figure 2).

### 3.1.1. *Autochthonous Variscan basement*

It is made up of a biotite and amphibole-bearing medium- to coarse-grained leucomonzogranite of about 305 Ma (Durand-Delga 1978; Amaudric du Chaffaut *et al.* 1985a,b; 'G2 calc-alkaline intrusives' in Paquette *et al.* 2003 and references therein).

### 3.1.2. *Parautochthonous units*

They correspond to a complex assemblage of subvertical N–S-trending thrust sheets of metamorphic mostly mylonitic terrains, derived from the Variscan basement and its Permian to Cretaceous-Eocene cover. They include: Variscan two-mica, garnet-bearing micaschists (Netelbeek 1951, 'roches brunes' in Termier and Maury 1928); sheared Carboniferous-Permian leucomonzogranite and diorite, acidic metavolcanics and metavolcanoclastites (mostly rhyolitic in composition) of likely Permian age; metaconglomerates with rhyolite and granite clasts of likely post-Berriasian age (Netelbeek 1951) and hosting a mixed sulphide ore body (Aicard *et al.* 1962 in Durand-Delga 1978).

### 3.1.3. *Schistes Lustrés*

These oceanic metamorphic rocks belong to the Schistes Lustrés Complex (Durand-Delga 1978, 1984) and, in particular, to the Inzecca Series (Amaudric du Chaffaut *et al.* 1972; Caron *et al.* 1979) or to the Inzecca Unit (Padoa 1999 and references therein). This almost complete oceanic succession, comprising both metaophiolites and their metasedimentary cover and spanning in age from Late Jurassic to Late Cretaceous (by correlation with the successions of the Northern Apennines and Western Alps, according to Amaudric du Chaffaut *et al.* 1972) includes, from bottom to top: serpentinized peridotites, ophicalcites and ophiolitic sandstones, pillow and massive basalts and pillow breccias, cherts and the Erbajolo Formation (phyllites with metacalcarenite and marble intercalations of likely Early Cretaceous age: Amaudric du Chaffaut *et al.* 1972).

## 3.2. *Structural and petrological data*

The data obtained from the meso-, micro-structural and petrographical studies are summarized in this paragraph, as well as the results of the chemical analyses performed on amphibole, lawsonite and white mica. Chemical data were obtained using a JEOL-FXA-8600 electron microprobe (Istituto di Geoscienze e Georisorse, CNR, Firenze, Italy), equipped with four wavelength-dispersive spectrometers and operating under the following conditions: 15 kV acceleration voltage, 15 s counting time, 10 nA excitation current, beam spots between 1 and 10  $\mu\text{m}$  in diameter (the largest spots were used on alkali-rich minerals, to avoid Na-K volatilization); the correction program by Bence and Albee (1968) was used. Additional analyses were performed using a WDS ARL-SEMQ electron microprobe (Dipartimento di Scienze della Terra, Università degli Studi di Modena e Reggio Emilia, Modena, Italy), equipped with four spectrometers and working under the following conditions: 15 kV acceleration potential, 10 nA beam current, 10 s counting time for each element plus 5 s for the background and beam spot diameters between 9  $\mu\text{m}$  and 15  $\mu\text{m}$  (the largest spots were used on alkali-rich minerals, to avoid Na-K volatilization). Data were acquired and elaborated using PROBE software by J. Donovan (Donovan *et al.* 1993). The results and re-calculations are shown in Tables 1 and 2 and in Figure 3 (a, b) and 5. In the diagrams (Figure 3a, b and 5) the literature data on the composition of amphiboles and phengites are also plotted for comparison.

The general structural framework of the Inzecca area, that is common to all the stacked units, is dominated by a N–S-trending, subvertical and very pervasive foliation, deformed by subsequent open to gentle folds, characterized by horizontal axial planes. Also, the tectonic contact between the Schistes Lustrés and the Parautochthonous Units displays a sub-vertical attitude and a weak later folding. In particular, the following polyphase structural and metamorphic framework can be recognized (Figure 4).

### 3.2.1. *Schistes Lustrés*

In these units, three deformative events (D1, D2 and D3), associated to three generations of folds and foliations (Figure 5), and a D4 brittle event have been recognized. The most evident structural feature in the field is the

Table 1. Representative microprobe analyses (wt%) of syn-D1 Na-amphiboles (structural formulae calculated assuming total cation sum minus Ca, Na, K = 13 per anhydrous formula unit)

Sample Lithotype	Blue-amphibole													OCG6II Granite	OCG6III Rhyolite			
	44	47	48	49	57	58	60	61	65	69	SP401IB Diorite	SP402IA Diorite	SP392IA Diorite					
wt%																		
SiO <sub>2</sub>	57.01	54.99	54.87	54.75	55.93	56.49	56.25	56.29	55.78	53.92	56.25	56.68	54.94	50.53	49.62			
TiO <sub>2</sub>	0.06	0.05	0.05	0.07	0.03	0.05	0.02	0.01	0.06	0.04	0.02	0	0.04	0.16	0.25			
Al <sub>2</sub> O <sub>3</sub>	2.74	2.72	4.33	3.24	1.82	4.01	4.28	3.66	3.01	2.30	3.735	3.15	2.535	0.44	0.84			
Cr <sub>2</sub> O <sub>3</sub>	0.03	0.00	0.02	0.00	0.01	0.02	0.00	0.02	0.02	0.00	0.03	0	0	0	0.05			
FeO	17.95	19.69	17.75	19.90	16.83	20.39	20.40	19.59	20.14	16.66	17.72	16.17	16.69	37.62	36.91			
MnO	0.26	0.21	0.25	0.22	0.29	0.20	0.16	0.22	0.28	0.33	0.11	0.14	0.2	0.29	0.2			
MgO	10.22	10.25	10.77	10.18	13.25	9.06	9.25	10.14	10.38	13.03	10.05	10.93	11.24	0.05	0.12			
CaO	3.78	3.41	4.49	2.36	6.95	1.79	1.62	2.84	2.84	6.73	1.91	3.76	5.32	0.05	0.08			
Na <sub>2</sub> O	4.98	5.47	4.58	6.47	3.64	6.65	6.72	5.83	6.18	3.43	5.25	4.7	4.03	6.88	6.86			
K <sub>2</sub> O	0.02	0.05	0.18	0.03	0.05	0.03	0.02	0.04	0.04	0.07	0	0.02	0.07	0.12	0.14			
Total	97.05	96.82	97.27	97.21	98.78	98.69	98.71	98.62	98.73	96.50	95.08	95.55	95.06	96.13	95.07			
Cations																		
Si	7.883	7.930	7.828	7.855	7.888	7.983	7.924	7.927	7.888	7.763	7.927	7.842	7.961	7.919	7.862			
Al <sup>(iv)</sup>	0.117	0.070	0.172	0.145	0.112	0.017	0.076	0.073	0.112	0.237	0.073	0.158	0.039	0.081	0.138			
Sum Z	8.000	8.000	8.000	8.000	8.000	8.000	8.000	8.000	8.000	8.000	8.000	8.000	8.000	8.000	8.000			
Al <sup>(vi)</sup>	0.628	0.392	0.555	0.402	0.190	0.650	0.634	0.534	0.390	0.153	0.704	0.692	0.476	0.001	0.019			
Ti	0.007	0.005	0.005	0.007	0.003	0.005	0.002	0.001	0.006	0.004	0.002	0.000	0.004	0.019	0.030			
Cr	0.003	0.000	0.002	0.000	0.001	0.003	0.000	0.002	0.002	0.000	0.003	0.000	0.000	0.000	0.006			
Fe <sup>2+</sup>	0.643	1.076	0.936	1.200	0.811	0.985	1.108	1.080	1.146	1.028	1.167	0.676	0.651	1.911	1.891			
Fe <sup>3+</sup>	1.507	1.298	1.181	1.187	1.173	1.424	1.294	1.227	1.235	0.977	0.959	1.270	1.391	3.019	2.999			
Mn	0.032	0.025	0.030	0.026	0.035	0.024	0.018	0.026	0.033	0.041	0.013	0.017	0.025	0.038	0.027			
Mg	2.181	2.203	2.291	2.178	2.786	1.909	1.942	2.130	2.188	2.796	2.150	2.345	2.452	0.012	0.028			
Sum Y	5.000	5.000	5.000	5.000	5.000	5.000	5.000	5.000	5.000	5.000	5.000	5.000	5.000	5.000	5.000			
Ca	0.580	0.527	0.686	0.363	1.050	0.271	0.245	0.428	0.430	1.038	0.294	0.580	0.834	0.008	0.014			
Na	1.383	1.473	1.265	1.637	0.950	1.729	1.755	1.572	1.570	0.957	1.461	1.311	1.143	1.992	1.986			
Sum X	1.963	2.000	1.951	2.000	2.000	2.000	2.000	2.000	2.000	1.995	1.754	1.891	1.977	2.000	2.000			
Na	0.000	0.055	0.000	0.162	0.045	0.093	0.080	0.019	0.125	0.000	0.000	0.000	0.000	0.099	0.121			
K	0.004	0.009	0.032	0.005	0.008	0.006	0.003	0.007	0.008	0.013	0.000	0.004	0.013	0.024	0.028			
Sum A	0.004	0.064	0.032	0.167	0.054	0.099	0.084	0.026	0.132	0.013	0.000	0.004	0.013	0.123	0.149			
Total	14.967	15.064	14.983	15.167	15.054	15.099	15.084	15.026	15.132	15.008	14.754	14.895	14.990	15.123	15.149			

Table 2. Representative microprobe analyses (wt%) of lawsonite (structural formulae calculated for 8 oxygens and assuming all Fe as Fe<sup>2+</sup>)

Sample Lithotype	Lawsonite			
	SP12b-1C Micaschist	SP12b-2C Micaschist	VEZ3-2C Rhyolite	VEZ3-2E Rhyolite
wt%				
SiO <sub>2</sub>	44.07	39.22	41.17	40.13
TiO <sub>2</sub>	0.03	0.02	0	0
Al <sub>2</sub> O <sub>3</sub>	28.05	29.92	29.19	28.73
FeO	0.16	0.2	0.48	0.96
MnO	0.08	0.00	0.08	0.06
MgO	0.01	0.00	0.11	0.47
CaO	15.21	15.89	16.17	15.33
Na <sub>2</sub> O	0.15	1.06	0.00	0.00
K <sub>2</sub> O	0.02	0.03	0.00	0.00
Total	87.78	89.34	90.2	88.68
Cations				
Si	2.283	2.097	2.168	2.154
Ti	0.001	0.001	0.00	0.00
Al	1.712	1.886	1.812	1.818
Fe <sup>3+</sup>	0.00	0.00	0.00	0.00
Fe <sup>2+</sup>	0.007	0.009	0.021	0.043
Mn	0.004	0.00	0.004	0.003
Mg	0.001	0.00	0.009	0.038
Ca	0.844	0.91	0.912	0.882
Na	0.015	0.11	0.00	0.00
K	0.001	0.002	0.00	0.00
Total	4.868	5.015	4.926	4.938

composite foliation, whose attitude has been determined by the D2 phase and that derives from the superposition of the axial plane foliations of the isoclinal and sub-coaxial D1 and D2 folds.

Given the strong transposition linked to the D2 phase, the previous structures (F1 isoclinal folds and S1 foliation) are quite rare and generally present as relics within S2 foliation. The infrequent F1 folds are intrafoliar, millimetric to centimetric, tight to isoclinal, with thickened angular hinges and thinned limbs, typical of the classes 2 and 3 of Ramsay (1967). Although S1 is rarely observable in the field, it is more frequently recorded in thin section (Figure 6), locally preserved in the microlithons of the S2 foliation, in the hinge zones of the F2 folds; here the superposition relationships between the S1 and S2 surfaces are still observable, because they intersect each other at a high angle, while in the other sectors these two surfaces are often indistinguishable, because the S1 is parallel to the axial planes of the F2 folds (Figure 6). S1 is made up of quartz, chlorite, phengite, albite, epidote and Mg-riebeckite (with Al<sup>VI</sup> comprised between 0.2 and 0.5) in the metabasalts and riebeckite+chlorite+jadeite/aegirine in the metaradiolarites (Netelbeek 1951). Undulose extinction and deformation lamellae in quartz porphyroclasts (Simpson 1985; Passchier and Trouw 1996) and type II and IV deformational twins in calcite (Burkhard 1993) are respectively observable in the quartzitic phyllites and metacalcarenite of the Erbjolo Formation. A mineral-stretching lineation L1, due to the isorientation of acicular or lamellar neo-formation minerals or formed by linear aggregates of pre-kinematic mineral grains (mainly quartz and calcite), occasionally occurs. L1 mainly plunges towards SW with angles ranging between 40° and 50° (Figure 7), but the data are quite scattered.

The D2 phase produced tight to isoclinal NW-verging folds, with generally thinned and boudinaged limbs, belonging to classes 2, 3 and locally 1B and 1C of Ramsay (1967). Their axes moderately plunge generally towards the western quarters and the axial planes are mostly NNW–SSE-striking with a steep, both westward and eastward,



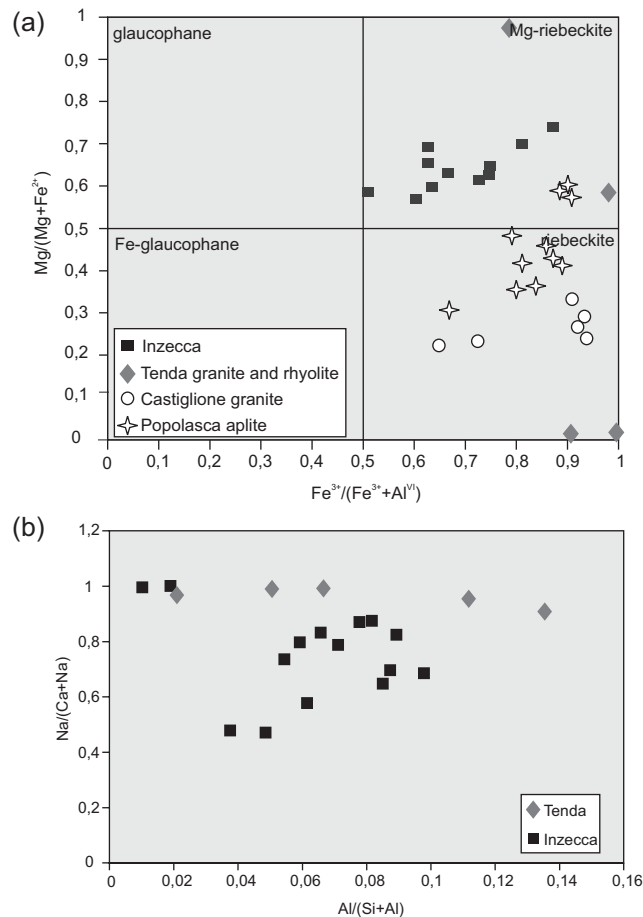


Figure 3. (a) Composition of syn-D1 Na-amphiboles within the Amphibole Diorite, the Rhyolite and the Sheared Granite (Parautochthonous Units) according to the classification of Leake *et al.* (1997). The data of the Inzecca-Ghisoni area are compared with the Na-amphibole literature data: from the Popolasca aplite (Malasoma *et al.* 2006), Tenda rhyolite and granite (Tribuzio and Giacomini 2002) and Castiglione parautochthonous granite (Morelli 2003) (b) Syn-D1 amphibole composition from the Amphibole Diorite, the Rhyolite and the Sheared Granite (Parautochthonous Units) of the Inzecca-Ghisoni area, compared with the literature data from the Tenda Massif high-pressure mineral assemblages (Tribuzio and Giacomini 2002).

dip (Figure 7). The S2 millimetric-spaced axial plane foliation (Figure 6) is constituted by greenschist facies mineral assemblages (albite+chlorite+sericite+epidote+tremolite in the metabasalts and chlorite+quartz+calcite+muscovite in the Erbjolo Formation), which determined the partial re-equilibration of the D1 paragenesis. A steeply-dipping L2 stretching lineation, generally striking NW–SE, is occasionally detectable (Figure 7), especially in the metabasalts, where it is underlined by the elongation of the pillows and of the associated variolitic texture. A more pervasive planar fabric characterizes a slice of stretched meta-pillow lavas occurring at the contact with the Parautochthonous Units.

The D3 phase produced only gentle to open, east-verging folds, often metric in size belonging to 1B and 1C classes of Ramsay (1967). F3 folds are characterized by mostly NNW–SSE-trending axes and sub-horizontal to 30° E-dipping axial planes (Figure 7). Their non-metamorphic, generally centimetrically- to decimetrically-spaced axial plane foliation (C3 = S3) is a gradational to discrete crenulation cleavage (outlined by reorientation of the phyllosilicates and by concentration of opaque minerals: Figure 6) or a disjunctive cleavage. In the Erbjolo Formation, the refraction of C3 is a typical feature, because of the alternation of more or less competent lithotypes.

The D4 phase consists of high-angle jointing and fault surfaces with ENE and W dip directions.

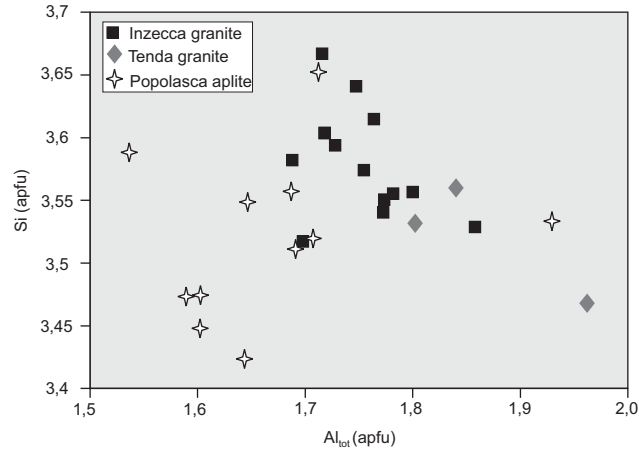


Figure 4. Composition of syn-D1 phengites from the Inzecca granite compared with the literature data: Tenda Massif granite according to Tribuzio and Giacomini (2002) and Popolasca aplite according to Malasoma *et al.* (2006).

### 3.2.2. Parautochthonous Units

Also these rocks are affected by three ductile deformative phases (D1, D2 and D3: Figure 5), followed by a brittle one (D4). The first two phases are syn-metamorphic and produce a peculiar composite mylonitic foliation. It is generally characterized by a sub-vertical attitude, an approximately NNW–SSE to N–S strike and a dip towards ENE, NW and SW. The deformation is heterogeneous within the Parautochthonous Units. In fact, it generally decreases from the eastern contact with the Schistes Lustrés towards the western contact with the almost unaffected monzogranite (Autochthonous Units), but may become intense along local shear zones. Such sheared rocks can be defined as protomylonites to ultramylonites, depending on the percentage of matrix relative to that of porphyroclasts (Spry 1969; Sibson 1977; Passchier and Trouw 1996).

The S1 continuous foliation (Figure 8) generally appears as an intrafoliar relic within the microlithons of the very transpressive mylonitic S2 planar fabric (Figure 9). In the micaschist, the S1 locally wraps around the pre-Alpine

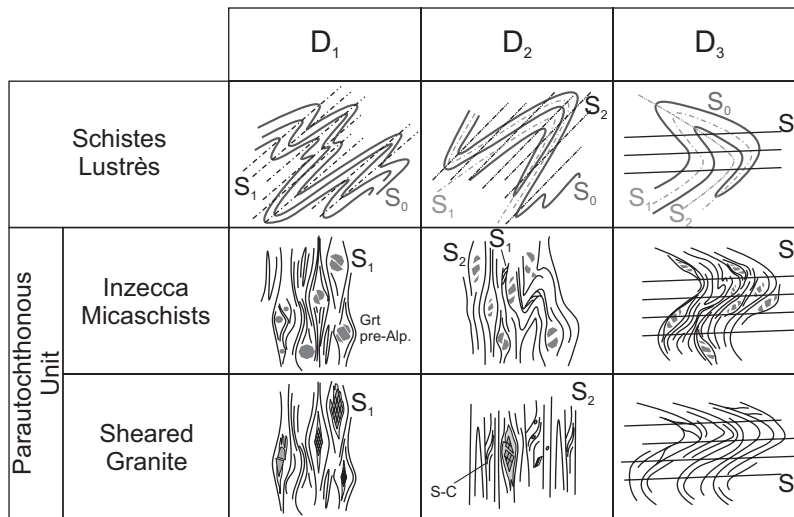


Figure 5. Alpine deformation evolution of the Schistes Lustrés and of the Parautochthonous Units.

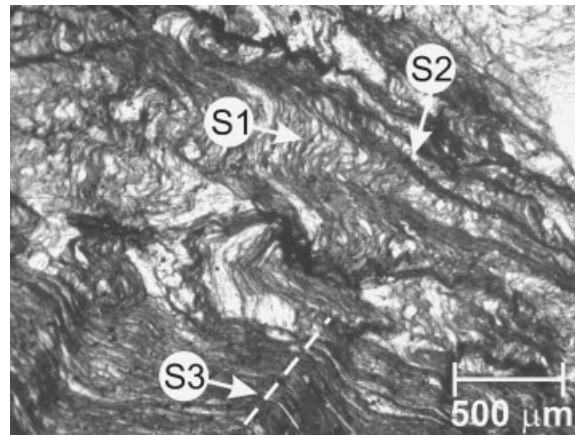


Figure 6. Photomicrograph of the Erabajolo Formation (Schistes Lustrés) showing superimposed S1, S2 and S3 foliations.

chloritized and broken garnet porphyroclasts and consists of phengite, chlorite and quartz. The static blastesis of lawsonite (Table 2) is widespread onto the plagioclase porphyroclasts. In the sheared monzogranite, S1 consists of celadonite-rich phengite ( $Si \approx 3.5\text{--}3.6$  apfu; Table 3), chlorite, quartz and Mg-riebeckite (static fibrous-radiate aggregates inside the quartz porphyroclasts and oriented ones in the pressure shadows; Figures 10a, 4a, 4b and Table 1). The quartz porphyroclasts show typical evidences of low-temperature crystal-plastic deformation, such as undulose extinction, grain size reduction and deformation lamellae, while K-feldspars display randomly oriented microfRACTURES (filled by neoblastic fine-grained albite) and undulose extinction (intracrystalline deformation at brittle/ductile boundary; Passchier and Trouw 1996). In the metarhyolite, S1 is formed by Mg-riebeckite, chlorite, phengite and quartz. The static blastesis of lawsonite has locally been observed onto plagioclase. In the metadiorite, S1 is made of epidote, quartz, phengite, albite and blue amphibole; this latter is mainly Mg-riebeckite (Figures 4a, 4b, 10b and Table 1), according to Leake *et al.* (1997) and grows in pressure shadows around magmatic hornblende.

The D2 structures are mylonitic shear zones and tight to isoclinal intrafoliar folds with axes trending averagely N–S. The D2 fabric elements are associated to a retro-metamorphic greenschist facies paragenesis, almost uniform in all the studied lithotypes and consisting of sericite-muscovite, albite, stilpnomelane, epidote, chlorite and winchite-barroisite or tremolite-actinolite (forming thin needles along the borders of blue-amphibole). The kinematic criteria (S/C structures,  $\sigma$ - and  $\delta$ -type porphyroblasts and strain fringes) point to an overall top-to-W or top-to-NW sense of shear (Figure 11). A L2 stretching lineation, plunging at high angle towards E, occasionally occurs, particularly in the metaconglomeratic lithotypes, where it is marked by the alignment of elongated clasts (Figure 8).

Also in the Parautochthonous Units, the D3 phase produced east-verging F3 gentle to open folds mostly with NNE–SSW- to N–S-trending sub-horizontal axes and sub-horizontal to  $30^\circ$  NE- to about E-dipping axial planes (Figure 8). The millimetric to metric-spaced sub-horizontal C3 axial plane cleavage has the same features of that observed in the Schistes Lustrés (Figure 9). It outlines the fact that the non-metamorphic D3 folding deformed also the contacts between the different tectonic slices, suggesting that they were already coupled during the D3 deformation in the Parautochthonous Units.

The brittle D4 event is represented by E-, NE- and W-trending high-angle joints and faults with little throw. In the sheared monzogranite, these structures cut previous NNW–SSE-trending joints and quartz veins.

### 3.2.3. Autochthonous Units

It generally shows no penetrative deformations at the meso- and micro-scale, but plurimetric Alpine (Amaudric du Chaffaut *et al.* 1985a,b) shear zones locally occur, also very far from the contact with the Parautochthonous Units

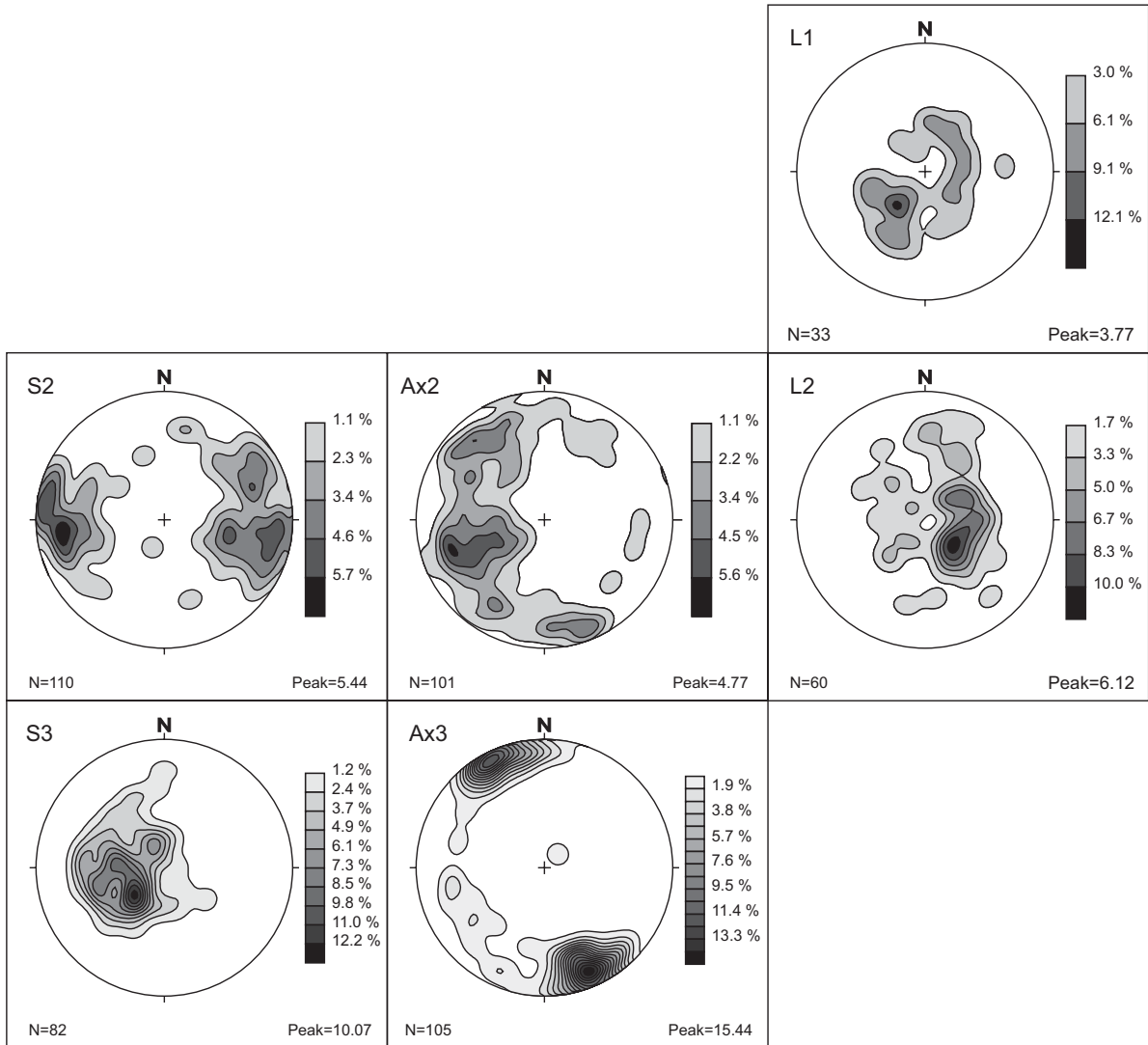


Figure 7. Stereographic representation of tectonic fabrics in the Schistes Lustrés (Schmidt's net, lower hemisphere). L1 and L2, mineral/stretching lineations; S2 and S3, foliations; Ax2 and Ax3, axial planes of folds.

(Monte d'Oro area, some tens of kilometres to the East of Ghisoni: Amaudric du Chaffaut *et al.* 1985a), which separate hectometric to kilometric portions of undeformed magmatic protolith. Along these bands the rock appears stretched and it acquires deformative features analogous to those described for the sheared granite; the contact with the almost unaffected protolith (monzogranite) tends to be a gradual fabric transition, from proto- to ultramyonites (Spry 1969; Sibson 1977; Shelley 1993; Passchier and Trouw 1996), ending in a granular texture.

#### 4. DISCUSSION

In this paper the Parautochthonous Units are considered to be slices of the Corse basement, involved in the Alpine deformations and metamorphism. In particular, the sheared granite and the associated metavolcanic and

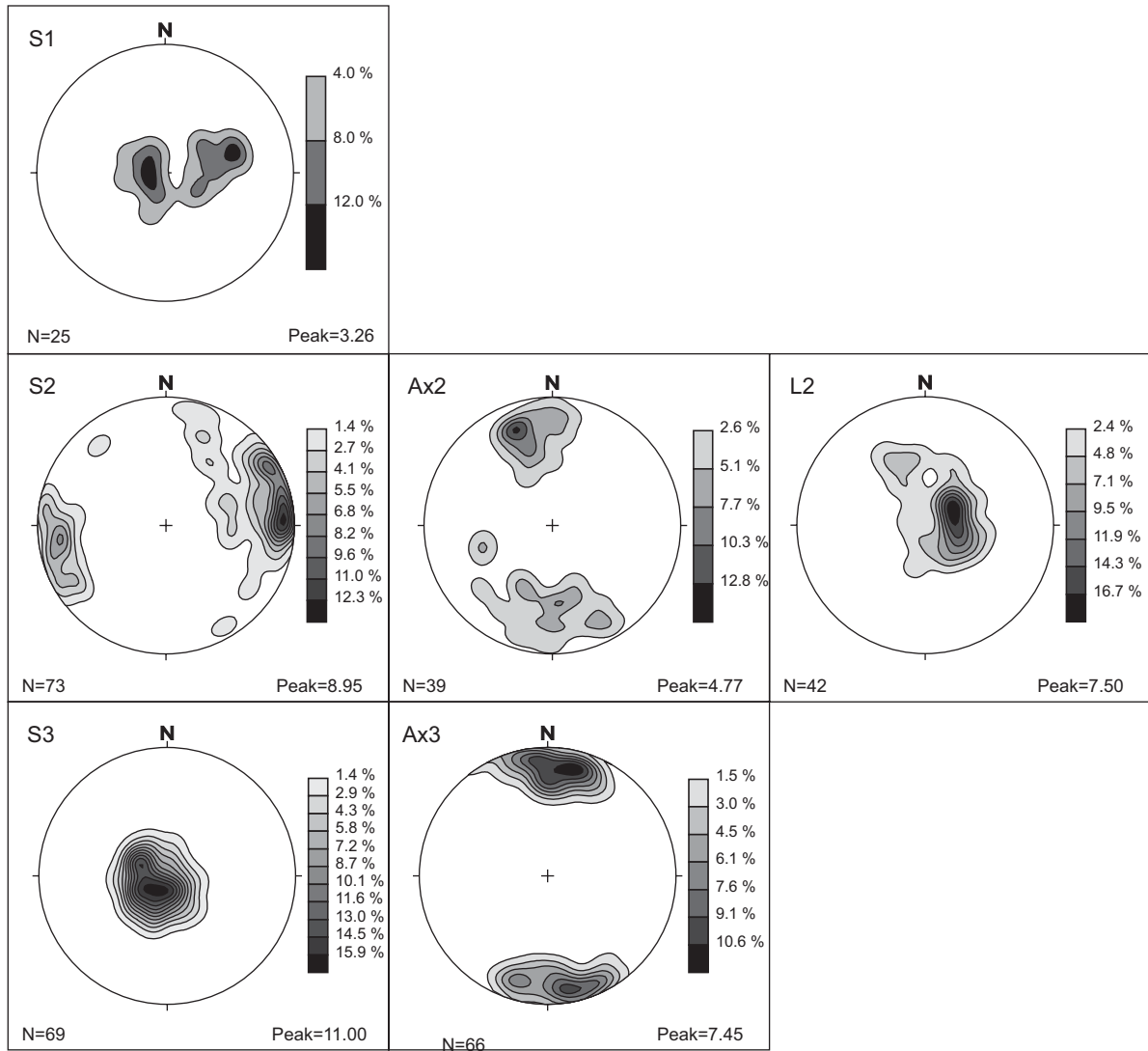


Figure 8. Stereographic representation of tectonic fabrics in the Parautochthonous Units (Schmidt's net, lower hemisphere).

metavolcanoclastic rocks are interpreted as the deformed equivalent of the adjacent autochthonous basement. Following Durand-Delga (1978), the garnet-bearing micaschists are considered to be remnants of the original host-rock of the batholith. Similar lithotypes ('garnet-bearing paragneiss and quartz-feldspathic granulites': Zibra 2006) were found also in the Santa Lucia Nappe to the north of Corte and variously interpreted: as Corsican/European Mesozoic continental margin according to Durand-Delga (1984 and references therein), as upper Austroalpine units from the Central Alps according to Caby and Jacob (2000), or as a lower crustal section exposed in the Ivrea Zone-Western Alps (Libourel 1988).

In the studied area both the Schistes Lustrés and the Parautochthonous Units show a polyphase deformation and metamorphic evolution, characterized by three main Alpine phases: D1, D2 and D3 (Figure 5). The deformative style of the first two syn-metamorphic phases (particularly D2) is different in the two ensembles of units. In fact, folds and axial plane foliations characterize the Schistes Lustrés, whereas shear zones and mylonitic foliations are

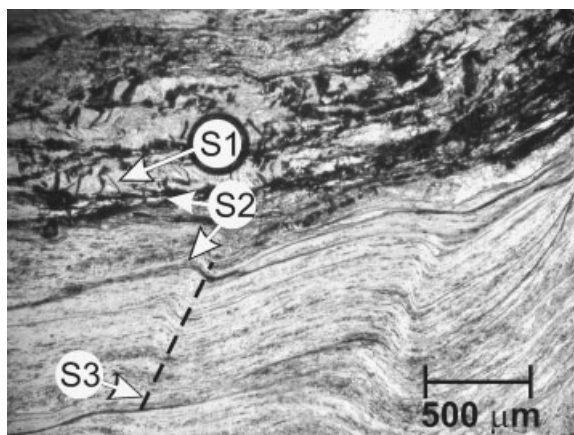


Figure 9. Photomicrograph of the Volcanic-Sedimentary Formation (Parautochthonous Units), showing superimposed S1, S2 and S3 foliations.

the typical structures in the Parautochthonous Units at the meso- and micro-scale. The following non-metamorphic D3 event caused only gentle to open folds with associated sub-horizontal axial plane cleavage in both the units. Moreover, both in the Schistes Lustrés and in the Parautochthonous Units, the tectonic transport is towards W or NW for the D2 phase, while the facing of the D3 folds is towards E.

Because of the strong transpositive effects of the D2 phase, the data about the D1 structural elements are scarce, but they suggest a ductile deformation and the development of a continuous foliation. In the Inzecca-Ghisoni sector, we found no unequivocal kinematic indicators for D1 in the studied rocks, but further to the north of this area and along the same structural alignment, other authors defined a top-to-W and top-to-SW sense of tectonic transport (Popolasca: Malasoma *et al.* 2006 and Tenda Massif: Molli and Tribuzio 2004; Molli *et al.* 2006. In the Schistes Lustrés, the observed syn-D1 paragenesis (Mg-riebeckite+chlorite) points to blue amphibole-greenschist metamorphic peak conditions (Padoa 1999). According to Simpson (1985) and Burkhard (1993) respectively, the deformational microfabrics observed in quartz and calcite porphyroclasts of the Erbajolo Formation suggest temperatures of deformation between 250°C and 300°C.

In the Parautochthonous Units the D1 event is associated to the development of a HP paragenesis including: Mg-riebeckite, celadonite-rich phengite, albite, quartz, chlorite and lawsonite. The previous authors recognized blue amphibole-bearing parageneses also in the corresponding Parautochthonous Units of the Corte area: riebeckite, both in the granitic basement and in the Mesozoic-Eocene metasedimentary cover (Bezert and Caby 1989), riebeckite+phengite in the matrix of the Cretaceous metaconglomerates and glaucophane in the metadoleritic dykes cross-cutting a slice of parautochthonous metagranite to the south of Corte (Durand-Delga 1978; Ritsema 1952), for which Maluski (in Amaudric du Chaffaut and Saliot 1979) obtained a  $^{39}\text{Ar}/^{40}\text{Ar}$  age of  $40 \pm 2$  Ma. According to Bezert (1990), the estimated P-T conditions for this event are 0.4–0.6 GPa and 320–410°C. Moreover, Malasoma *et al.* (2006) estimated  $P = 0.50\text{--}0.80$  GPa and  $T = 300\text{--}370$ °C, for mineralogical associations and microfabrics analogous to those found in the Inzecca-Ghisoni area and attributed them to low-grade blueschist facies. Similar compositions were found for syn-D1 blue amphiboles in the parautochthonous granite at Castiglione, to the north of Corte (unpublished data by Morelli 2003). In the Popolasca area (north of Corte), the occurrence of Bartonian nummulites in the parautochthonous metaconglomerates (Bezert and Caby 1989) and the apatite fission track data (Fellin *et al.* 2005 and references therein) constrain the D1 event to a short time span between Late Eocene and Early Oligocene (between 40–37 and 30 Ma). These data agree with the  $^{39}\text{Ar}/^{40}\text{Ar}$  age of  $40 \pm 2$  Ma (Late Eocene), obtained by Maluski (in Amaudric du Chaffaut and Saliot 1979) for the blue-amphiboles in the doleritic dykes of Corte.

Thus, we refer the D1 phase to the Late Eocene underplating and accretion in a subduction zone both of the residual oceanic lithosphere and of part of the European margin.

Table 3. Representative microprobe analyses (wt%) of syn-D1 phengite (structural formulae calculated for 11 oxygens and assuming all Fe as Fe<sup>2+</sup>)

Sample Lithotype	Phengite											OCG6m4 Granite			
	75 Granite	77 Granite	78 Granite	79 Granite	81 Granite	85 Granite	86 Granite	88 Granite	109 Granite	110 Granite	OCG4m1 Granite		OCG5m2 Granite		
wt%															
SiO <sub>2</sub>	50.21	51.51	51.75	51.48	52.34	52.41	52.35	50.90	53.86	54.34	51.66	52.51	51.46		
TiO <sub>2</sub>	0.09	0.05	0.06	0.02	0.04	0.04	0.06	0.04	0.03	0.04	0.05	0.06	0.09		
Al <sub>2</sub> O <sub>3</sub>	20.54	20.62	22.00	21.85	22.19	21.37	22.46	22.75	21.94	21.58	21.5	21.24	21.3		
FeO	10.21	7.96	7.20	7.59	7.72	8.05	6.66	6.26	6.83	7.35	6.11	6.15	6.34		
MnO	0.15	0.12	0.06	0.08	0.01	0.11	0.17	0.11	0.14	0.13	0.01	0.17	0.13		
MgO	3.37	3.13	3.10	2.95	2.90	2.55	2.95	2.72	2.26	1.98	3.25	3.43	3.02		
CaO	0.03	0.02	0.06	0.04	0.06	0.02	0.04	0.08	0.03	0.09	0.06	0.04	0		
Na <sub>2</sub> O	0.09	0.01	0.01	0.03	0.05	0.06	0.06	0.05	0.05	0.02	0.02	0	0		
K <sub>2</sub> O	9.918	11.17	10.818	11.544	11.53	10.9	11.28	11.17	10.89	10.58	11.77	11.25	11.4		
Cr <sub>2</sub> O <sub>3</sub>	0.01	0.03	0.00	0.00	0.01	0.00	0.01	0.00	0.01	0.00	0.003	0.012	0.03		
Total	94.62	94.62	95.05	95.57	96.84	95.51	96.04	94.08	96.04	96.10	94.43	94.85	93.77		
Cations															
Si	3.517	3.582	3.554	3.543	3.549	3.596	3.557	3.528	3.639	3.668	3.575	3.604	3.614		
Al <sup>(iv)</sup>	0.483	0.418	0.446	0.457	0.451	0.404	0.443	0.472	0.361	0.332	0.425	0.397	0.386		
sum Z	4.000	4.000	4.000	4.000	4.000	4.000	4.000	4.000	4.000	4.000	4.000	4.000	4.000		
Al <sup>(vi)</sup>	1.213	1.272	1.335	1.315	1.322	1.324	1.355	1.385	1.387	1.385	1.328	1.321	1.377		
Ti	0.005	0.003	0.003	0.001	0.002	0.002	0.003	0.002	0.001	0.002	0.003	0.003	0.000		
Fe <sup>2+</sup>	0.599	0.464	0.414	0.437	0.438	0.462	0.379	0.363	0.386	0.415	0.354	0.353	0.373		
Mn	0.009	0.007	0.003	0.004	0.000	0.006	0.010	0.007	0.008	0.007	0.001	0.010	0.008		
Mg	0.352	0.325	0.318	0.302	0.293	0.261	0.298	0.281	0.227	0.199	0.335	0.351	0.237		
Cr	0.001	0.002	0.000	0.000	0.000	0.000	0.001	0.000	0.000	0.000	0.000	0.000	0.001		
sum Y	2.178	2.072	2.073	2.059	2.056	2.056	2.045	2.038	2.010	2.008	2.021	2.039	1.995		
Ca	0.002	0.001	0.004	0.003	0.004	0.001	0.003	0.006	0.002	0.006	0.004	0.003	0.000		
Na	0.013	0.002	0.001	0.003	0.006	0.008	0.008	0.007	0.007	0.002	0.003	0.000	0.000		
K	0.887	0.991	0.948	1.014	0.998	0.955	0.978	0.987	0.939	0.912	1.039	0.985	1.022		
sum X	0.902	0.994	0.954	1.020	1.008	0.964	0.989	1.000	0.948	0.920	1.046	0.988	1.022		
Total	7.079	7.066	7.027	7.079	7.064	7.020	7.034	7.039	6.958	6.928	7.067	7.027	7.016		

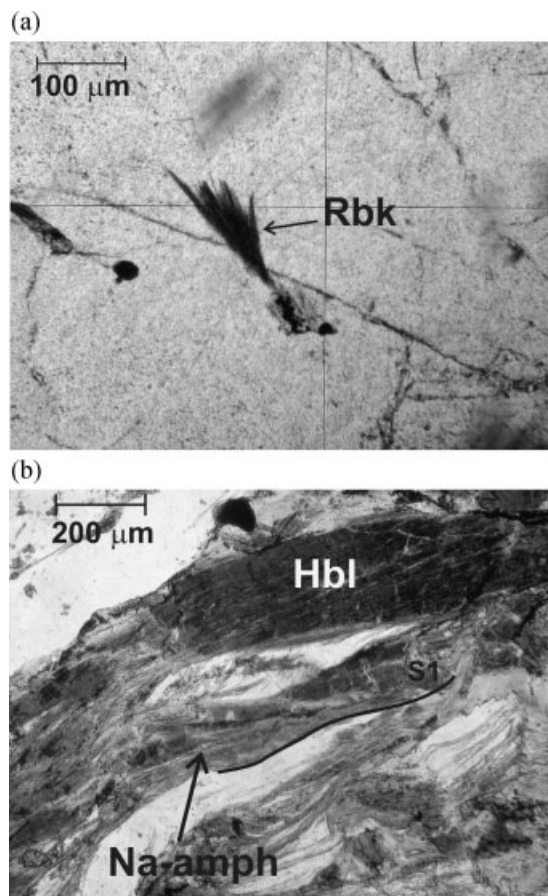


Figure 10. (a) Fan-shaped Na-amphibole (Riebeckite = Rbk) within a quartz porphyroclast in the Sheared Granite. (b) Photomicrograph of the Amphibole Diorite (Parautochthonous Units). Syn-D1 Na-amphibole (crossite) growth around a Hbl porphyroclast (S1 = S1 foliation).

The following D2 greenschist facies event is likely referable to the exhumation of the HP units towards shallow depths. The P-T conditions of the D2 metamorphism in the units of the Alpine Corsica have been generally estimated in  $P \leq 0.5$  GPa and  $T \leq 350$ – $450^\circ\text{C}$  (Ohnenstetter *et al.*, 1976; Lahondère 1991; Molli and Tribuzio 2004 and references therein).

The data arising from the studied area show that the D2 event produced the retrograde re-equilibration of the previous HP paragenesis in the greenschist facies and a different ductile imprint in the units occurring at different structural levels: tight to isoclinal folding in the Schistes Lustrés, whereas slicing and mylonitic shearing dominate in the Parautochthonous Units, and also in some metric shear zones recognized within the autochthonous monzogranite. All the D2 kinematic indicators, such as S/C/C'-type shear bands and mantled porphyroclasts ( $\delta$ - or  $\sigma$ - objects) of quartz and feldspar, point to a westward vergence, which testifies to the overthrusting of the Alpine Corsica pile of nappes onto the Variscan Corsica margin, that suffered ductile shearing. Instead, other authors found a mostly top-to-NE sense (and locally also top-to-W and top-to-SW sense) of the tectonic transport during D2 in the corresponding units along the same structural alignment (Tenda Massif: Molli and Tribuzio 2004; Molli *et al.* 2006 and references therein). Jolivet *et al.* (1990, 1991) and Daniel *et al.* (1996) interpreted the eastward vergence of the greenschist phase as the effect of conjugate sets of ductile shear bands active in a 'Core Complex'-like post-collisional extensional setting. We think that these coexisting opposite senses can be related to a composite nature



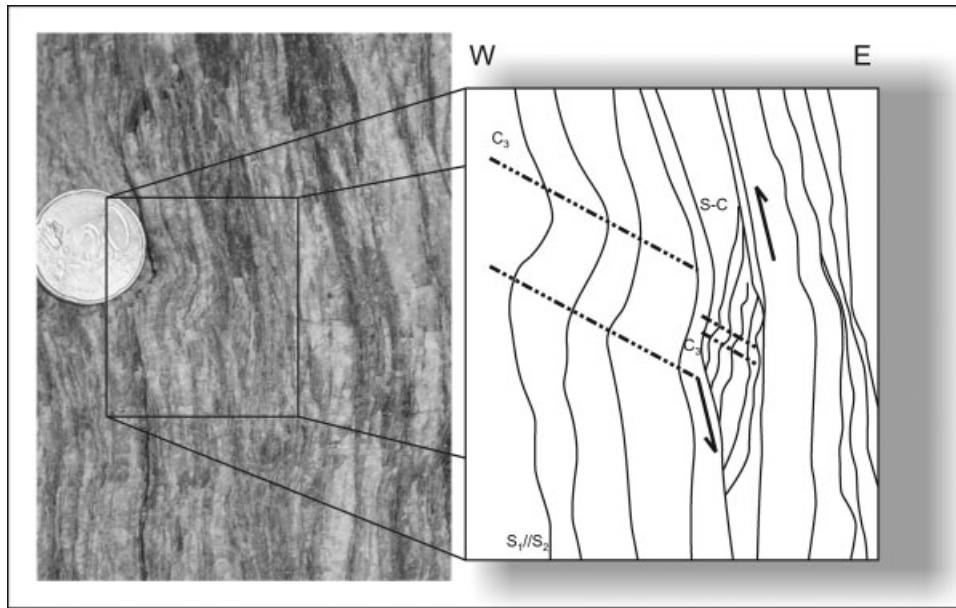


Figure 11. D2 top-to-W sense of shear indicator in the Sheared Granite, along S1//S2 foliation, deformed by later C3 crenulations.

of the D2 event and, in particular, to back-thrusting and folding related to syn-collisional extensional tectonics active during the general westward piling up and exhumation of the Alpine units onto the Variscan Corsica, as also suggested by other authors (Harris 1985; Warburton 1986; Padoa 1999; Molli *et al.* 2006). The D2 is radiometrically well constrained for the Tenda Massif in the 35–25 Ma time interval (Brunet *et al.* 2000,  $^{40}\text{Ar}/^{39}\text{Ar}$  method on phengites), pointing to a very short time span elapsing between the HP Late Eocene accretion of the oceanic and continental units and their Oligocene syn-collisional exhumation.

The present tectonic juxtaposition of the Schistes Lustrés onto the Parautochthonous Units likely happened before the D3 phase and maybe during the latest stages of the D2 event, as suggested by the following structural considerations: (a) rocks belonging to the two different domains (allochthonous and parautochthonous) are never found folded together in a D1 or D2 structure; (b) the contact between these units is represented by a sharp surface, deformed by the F3 folds; (c) there is no evidence of tectonic slices of one unit in the other and (d) the slice of metabasalts, interposed between the Erhajolo Formation (Schistes Lustrés) and the Inzecca Micaschists (Parautochthonous Unit) (Figure 2), is characterized by a deformative pattern very similar to that of Parautochthonous Units, with the pillows that appear stretched and elongated parallel to the contact, forming lens-shaped bodies, wrapped by a pervasive subvertical foliation, developed in the recrystallized hyaloclastitic matrix and deformed by the D3 folds. Thus, we hypothesize a progressive temporal and spatial evolution of the D2 phase (Figure 12) with the development of folds and axial plane foliations in the Schistes Lustrés during their exhumation and thrusting onto the already deformed and HP/LT metamorphosed edge of the European (Corsica) margin; this latter area, together with the nearby portion of Schistes Lustrés, was affected mostly by ductile slicing and shearing, acquiring its peculiar mylonitic fabric (D2\* phase in Figure 12). Nevertheless, the petrographical data do not completely corroborate this interpretation: in fact, the different mineralogical assemblages associated to the D2 phase in the metaophiolites and in the parautochthonous crustal slices suggest almost different thermo-baric conditions for the D2 phase in the two units.

The non-metamorphic D3 event determined a east-vergent gentle to open folding and possibly the verticalization of the tectonic contacts between the main units (and inside them); it can be connected to the later deformation event in the brittle-ductile transition, which originated large-scale folds (e.g. the Cap Corse-Castagniccia megafold) and

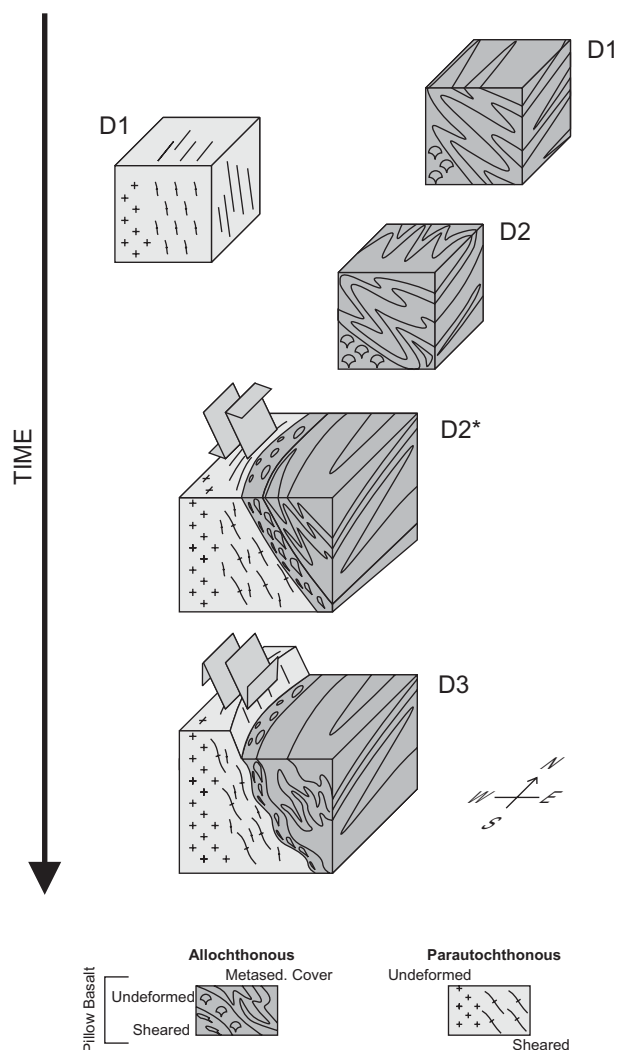


Figure 12. Sketch showing the time relations between D1, D2 and D3 and tectonic coupling of Parautochthonous and Autochthonous Units.

faulting at a regional scale. This event is referred to the post-orogenic extensional (Daniel *et al.* 1996; Brunet *et al.* 2000 and references therein) or transtensive (Molli and Tribuzio 2004; Molli *et al.* 2006) activity, which affected the Alpine Corsica tectonic pile during the Miocene.

Finally, the brittle D4 event produced high-angle faulting and jointing in the rocks of the Inzecca-Ghisoni transect.

## 5. CONCLUSIONS

The study of the Alpine units along the Inzecca-Ghisoni transect demonstrates that the continuous belt of continental slices, characterized by HP/LT metamorphism of Tertiary age, extending from the Tenda Massif to Corte, envisaged by previous authors (Gibbons and Horak 1984; Bezert and Caby 1988, 1989; Tribuzio and

Giacomini 2002; Molli and Tribuzio 2004; Malasoma *et al.* 2006; Molli *et al.* 2006; Malasoma and Marroni 2007), continues also southwards and reaches the Inzecca area. That is, almost all the eastern border of the European margin in Corsica has been affected, during Tertiary age, by HP metamorphism and deformations. This implies a history of burial and exhumation during the Alpine orogenesis, which caused juxtaposition between various metamorphic oceanic units and the undeformed continental basement, through the interposition of HP-metamorphic continental-derived parautochthonous units.

#### ACKNOWLEDGEMENTS

This research was sponsored by the Italian Ministry for University and Scientific and Technological Research (M.I.U.R.-COFIN). Prof. Riccardo Tribuzio (University of Pavia, Italy), Prof. Philippe Rossi (BRGM, Orléans, France) and Prof. Michele Marroni (University of Pisa, Italy) are thanked for the very useful comments and suggestions, which substantially improved the original submitted manuscript. Dr. Chiara Petrone and Dr. Simona Bigi are acknowledged for electron microprobe analyses.

#### REFERENCES

- Amaudric du Chaffaut S, Caron JM, Delcey R, Lemoine M. 1972.** Données nouvelles sur la stratigraphie des Schistes Lustrés de Corse : la série de l'Inzecca. Comparaisons avec les Alpes Occidentales et l'Apennin ligure. *Comptes-Rendus de l'Académie des Sciences de Paris D*. **275**: 2611–2614.
- Amaudric du Chaffaut S, Kienast JR, Saliot P. 1976.** Répartition de quelques minéraux du métamorphisme Alpine en Corse. *Bulletin de la Société Géologique de France* **18**: 1153–1230.
- Amaudric du Chaffaut S, Saliot P. 1979.** La région de Corte: secteur clé pour la compréhension du métamorphisme alpin en Corse. *Bulletin de la Société Géologique de France* **21**(2): 149–154.
- Amaudric du Chaffaut S. 1982.** *Les Unités Alpines à la Marge Orientale du Massif Cristallin Corse*. Presses de l' Ecole Normale Supérieure: Paris.
- Amaudric du Chaffaut S, Bonin B, Caron JM, Conchon O, Rossi P. 1985a.** *Carte Géologique de la France (1/50000), feuille Venaco (1114)*. B.R.G.M: Orléans, France.
- Amaudric du Chaffaut S, Bonin B, Caron JM, Conchon O, Rossi P. 1985b.** *Notice explicative, Carte Géologique de la France (1/50000), feuille Venaco(1114)*. B.R.G.M: Orléans, France.
- Bence AE, Albee AL. 1968.** Empirical correction factors for the electron microanalysis of silicate and oxides. *Journal of Geology* **76**: 382–403.
- Bezert P. 1990.** *Les unités Alpines de la marge du Massif Cristallin Corse: Nouvelles données structurales, métamorphiques et contraintes cinématiques*. Thèse de 3<sup>ème</sup> cycle, Univ. Montpellier II, France.
- Bezert P, Caby R. 1988.** Sur l'âge post-bartonien des événements tectono-métamorphiques alpins en bordure orientale de la Corse cristalline (Nord de Corte). *Bulletin de la Société Géologique de France* **8**, IV: 965–971.
- Bezert P, Caby R. 1989.** La déformation progressive de l'Eocène de la région de Corte: nouvelles données petrostructurales et conséquences pour la tectogenèse Alpine en Corse. *Comptes-Rendus de l'Académie des Sciences de Paris* **309**(II): 95–101.
- Bortolotti V, Fazzuoli M, Pandeli E, Principi G, Babbini A, Corti S. 2001.** Geology of Central and Eastern Elba Island, Italy. *Ophioliti* **26**(2a): 97–150.
- Brunet C, Monié P, Jolivet L, Cadet JP. 2000.** Migration of compression and extension in the Tyrrhenian Sea, insight from <sup>40</sup>Ar/<sup>39</sup>Ar ages on micas along a transect from Corsica to Tuscany. *Tectonophysics* **321**: 127–155.
- Burkhard M. 1993.** Calcite-twins, their geometry, appearance and significance as stress-strain markers and indicators of tectonic regime: a review. *Journal of Structural Geology* **15**: 351–368.
- Caby R, Jacob C. 2000.** La transition croûte-manteau dans la nappe de Santa-Lucia-di-Mercurio (Corse Alpine): les racines d'un rift permien. *Géologie de la France* **1**: 21–34.
- Caron JM. 1994.** Metamorphism and deformation in Alpine Corsica. *Schweizerische Mineralogische und Petrographische Mitteilungen* **74**: 105–114.
- Caron JM, Delcey R, Scius H, Esseïn JP, Fraipont P, Mawhin B, Reuber I. 1979.** Répartition cartographique des principaux types des séries dans les Schistes Lustrés de Corse. *Comptes-Rendus de l'Académie des Sciences de Paris* **288**: 1363–1366.
- Caron JM, Péquignot G. 1986.** The transition between blueschist and lawsonite-bearing eclogites based on observations from Corsican metabasalts. *Lithos* **19**: 205–218.
- Cavazza W, DeCelles PG, Fellin MG, Paganelli L. 2007.** The Miocene Saint Florent Basin in northern Corsica: stratigraphy, sedimentology and tectonic implications. *Basin Research* **19**: 507–527.
- Cocherie A, Rossi P, Fanning CM, Guerrot C. 2005.** Comparative use of TIMS and SHRIMP for U-Pb zircon dating of A-type granites and mafic tholeiitic layered complexes and dykes from the Corsican Batholith (France). *Lithos* **82**: 185–219.

- Dallan L, Puccinelli A. 1995.** Geologia della regione tra Bastia e Saint-Florent (Corsica settentrionale). *Bollettino della Società Geologica Italiana* **114**: 23–66.
- Daniel JM, Jolivet L, Goffé B, Poisson C. 1996.** Crustal-scale strain partitioning. Footwall deformation below the Alpine Corsica Oligo-Miocene detachment. *Journal of Structural Geology* **18**: 41–59.
- Donovan JJ, Snyder DA, Rivers ML. 1993.** An improved interference correction for trace element analysis. *Microbeam Analysis* **2**: 23–28.
- Durand-Delga M. 1978.** *Corse. Guides géologiques régionaux*. Masson: Paris.
- Durand-Delga M. 1984.** Principaux traits de la Corse Alpine et correlations avec les Alpes Ligures. *Memorie della Società Geologica Italiana* **28**: 285–329.
- Egal E. 1992.** Structures and tectonic evolution of the external zone of Alpine Corsica. *Journal of Structural Geology* **14**: 1215–1228.
- Elter FM, Pandeli E. 2005.** Structural-metamorphic correlations between three Variscan segments in Southern Europe: Maures Massif (France), Corsica (France)-Sardinia (Italy), and Northern Apennines (Italy). In *The Southern Variscan Belt, Journal of the Virtual Explorer*, Carosi R, Dias R, Iacopini D, Rosenbaum G (eds). Electronic Edition, ISSN 1441–8142, **19**, Paper 1.
- Faccenna C, Mattei M, Funicello R, Jolivet L. 1997.** Styles of back-arc extension in the central Mediterranean. *Terra Nova* **9**: 126–130.
- Faure M, Malavieille J. 1981.** Étude structurale d'un cisaillement ductile: le charriage ophiolitique corse dans la région de Bastia. *Bulletin de la Société Géologique de France* **7**: 335–343.
- Fellin MG, Picotti V, Zattin M. 2005.** Neogene to Quaternary rifting and inversion in Corsica: retreat and collision in the western Mediterranean. *Tectonics* **24**: TC1011. DOI:10.1029/2003TC001613
- Ferrandini M, Ferrandini J, Loy e-Pilot MD, Butterlin J, Cravette J, Janin MC. 1998.** Le Miocene du Bassin de Saint-Florent (Corse): modalités de la transgression du Burdigalien Supérieur et mise en évidence du Serravallien. *Geobios* **31**: 125–137.
- Gibbons W, Horak J. 1984.** Alpine metamorphism of Hercynian hornblende granodiorite beneath the blueschist-facies Schistes Lustrés nappe of NE Corsica. *Journal of Metamorphic Geology* **2**: 95–113.
- Harris LB. 1985.** Progressive and polyphase deformation of the Schistes Lustrés in Cap Corse, Alpine Corsica. *Journal of Structural Geology* **7**(6): 637–650.
- Jolivet L, Faccenna C, Goffé B, Mattei M, Rossetti F, Brunet C, Storti F, Funicello C, Cadet JP, Parra T. 1998.** Mid crustal shear zones in post-orogenic extension: the northern Tyrrhenian Sea case. *Journal of Geophysical Research* **103**(6): 12123–12160.
- Jolivet L, Dubois R, Fournier M, Goffé B, Michard A, Jourdan C. 1990.** Ductile extension in Alpine Corsica. *Geology* **18**: 1007–1010.
- Jolivet L, Daniel JM, Fournier M. 1991.** Geometry and kinematics of extension in Alpine Corsica. *Earth and Planetary Science Letters* **104**: 278–291.
- Lahondère D. 1988.** Le métamorphisme écolitique dans les orthogneiss et les metabasites ophiolitiques de la région de Farinole. *Bulletin de la Société Géologique de France* **8**: 579–585.
- Lahondère D. 1991.** *Les Schistes bleu et les éclogetes à lawsonite des unités continentales et océaniques de la Corse Alpine: nouvelles données pétrologiques et structurales*. Thèse Doct., Univ. De Montpellier, France.
- Lahondère D, Guerrot C. 1997.** Datation Sm/Nd du métamorphisme écolitique en Corse Alpine, un argument pour l'existence, au Crétacé supérieur, d'une zone de subduction active localisée le long du bloc coso-sarde. *Géologie de la France* **3**: 3–11.
- Leake BE, Wooley AR, Arps CES, Birch WD, Gilbert MC, Grice JD, Hawthorne FC, Kato A, Kisch HJ, Krivivichev VG, Linthout K, Laird J, Mandarino JA, Maresch WV, Nickel EH, Rock NMS, Schumacher JC, Smith DC, Stephenson NCN, Ungaretti L, Whittaker E, Youzhi G. 1997.** Nomenclature of amphiboles: report of the subcommittee on amphiboles of the International Mineralogical Association Commission on New Minerals and Minerals Names. *Mineralogical Magazine* **61**: 259–321.
- Libourel G. 1988.** Le complexe de Santa-Lucia di Mercurio (Corse): un Nouveau jalon de la base de la croûte varisque en Méditerranée occidentale. *Comptes-Rendus de l'Académie des Sciences de Paris* **307**(II): 1067–1073.
- Malasoma A, Marroni M. 2007.** HP/LT metamorphism in the Volparone Breccia (Northern Corsica, France): evidence for involvement of the Europe/Corsica continental margin in the Alpine subduction zone. *Journal of Metamorphic Geology* **25**(5): 529–545.
- Malasoma A, Marroni M, Musumeci G, Pandolfi L. 2006.** High-pressure mineral assemblage in granitic rocks from continental units, Alpine Corsica, France. *Geological Journal* **41**(1): 49–59.
- Malavieille J, Chemenda A, Larroque C. 1998.** Evolutionary model for Alpine Corsica: mechanism for ophiolite emplacement and exhumation of high-pressure rocks. *Terra Nova* **10**: 317–322.
- Maluski H. 1977.** *Application de la méthode  $^{40}\text{Ar}/^{39}\text{Ar}$  aux minéraux des roches cristallines perturbées par des événements thermiques et tectoniques en Corse*. Thèse d'Etat, Univ. Montpellier, France.
- Marroni M, Pandolfi L. 2003.** Deformation history of the ophiolite sequence from the Balagne Nappe, northern Corsica: insights in the tectonic evolution of Alpine Corsica. *Geological Journal* **38**(1): 67–83.
- Mattauer M, Proust F, Etchecopar A. 1977.** Linéations 'a' et mécanisme de cisaillement simple liés au chevauchement de la nappe des Schistes lustrés en Corse. *Bulletin de la Société Géologique de France* **7**(XIX): 841–847.
- Mattauer M, Faure M, Malavieille J. 1981.** Transverse lineation and large-scale structures related to Alpine obduction in Corsica. *Journal of Structural Geology* **3**: 401–409.
- Menot RP, Orsini JB. 1990.** Evolution du socle ante-stephaniende Corse: événements magmatiques et métamorphiques. *Schweizerische Mineralogische und Petrographische Mitteilungen Bulletin* **70**: 35–53.
- Molli G, Tribuzio R. 2004.** Shear zones and metamorphic signature of subducted continental crust as tracers of the evolution of the Corsica/Northern Apennine orogenic system. In *Flow Processes in Faults and Shear Zones*, Alsop GI, Holdsworth RE, McCaffrey KJW, Hand M (eds). Geological Society of London: London; Special Publication: **224**; 321–335.
- Molli G, Tribuzio, Marquer D. 2006.** Deformation and metamorphism at the eastern border of the Tenda Massif (NE Corsica): a record of subduction and exhumation of continental crust. *Journal of Structural Geology* **28**: 1748–1766.
- Morelli G. 2003.** *Studio geologico, strutturale e petrologico delle unità metamorfiche e dei granitoidi associati affioranti tra Popolasca e Ponte Castirla (Corsica centro-settentrionale)*. Ph. D. Thesis, Università degli Studi di Firenze, Italy.
- Netelbeek TAF. 1951.** *Géologie et pétrologie de la région entre Vezzani et Lugo di Nazza*. Thèse Inst. Geol. Amsterdam, Netherlands.

- Ohnenstetter D, Ohnenstetter M, Rocci G. 1976.** Étude des métamorphismes successifs des cumulates ophiolitiques de Corse. *Bulletin de la Société Géologique de France* **18**: 115–134.
- Padoa E. 1999.** Les ophiolites du massif de l'Inzecca (Corse Alpine): litostratigraphie, structure géologique et évolution géodynamique. *Géologie de la France* **3**: 37–48.
- Paquette JL, Ménot RP, Pin C, Orsini JB. 2003.** Episodic and short lived granitic pulses in a post-collisional setting: evidence from precise U-Pb zircon dating through a crustal cross-section in Corsica. *Chemical Geology* **198**: 1–20.
- Passchier CW, Trouw RAJ. 1996.** *Microtectonics, (2nd corrected reprint)*. Springer-Verlag: Berlin Heidelberg.
- Ramsay JG. 1967.** *Folding and Fracturing of Rocks*. McGraw-Hill: New York.
- Ritsema L. 1952.** *Géologie de la région de Corte(Corse)*. Thèse no. 196, Amsterdam, Netherlands.
- Shelley D. 1993.** *Igneous and Metamorphic Rocks Under the Microscope*. Chapman and Hall: London.
- Sibson RH. 1977.** Fault rocks and fault mechanisms. *Journal of the Geological Society of London* **133**: 191–213.
- Simpson C. 1985.** Deformation of granitic rocks across the brittle-ductile transition. *Journal of Structural Geology* **7**: 503–511.
- Speranza F, Villa IM, Sagnotti L, Florindo F, Cosentino D, Cipollari P, Mattei M. 2002.** Age of the Corsica-Sardinia rotation and Liguro-Provençal Basin spreading: new paleomagnetic and Ar/Ar evidence. *Tectonophysics* **347**: 231–251.
- Spry A. 1969.** *Metamorphic Textures*. Pergamon Press: Oxford.
- Termier P, Maury E. 1928.** Nouvelles observations géologiques dans la Corse orientale. *Comptes-Rendus de l'Académie des Sciences de Paris* **186**: 1324–1327, 1393–1396.
- Tribuzio R, Giacomini F. 2002.** Blueschist facies metamorphism of peralkaline rhyolites from the Tenda crystalline massif (northern Corsica): evidence for involvement in the Alpine subduction event? *Journal of Metamorphic Geology* **20**(5): 513–526.
- Warburton J. 1986.** The ophiolite-bearing Schistes Lustrés nappe in Alpine Corsica: a model for the emplacement of ophiolites that have suffered HP/LT metamorphism. *Geological Society of America Memoir* **164**: 313–331.
- Zarki-Jakni B, Van der Beek P, Poupeau G, Sosson M, Labrin E, Rossi P, Ferrandini J. 2004.** Cenozoic denudation of Corsica in response to Ligurian and Tyrrhenian extension: results from apatite fission track thermochronology. *Tectonics* **23**: TC1003. DOI: 10.1029/2003TC001535
- Zibra I. 2006.** *Late-Hercynian granitoid plutons emplaced along a deep crustal shear zone. A case study from the S. Lucia Nappe (Alpine Corsica, France)*. Ph.D. Thesis, Università degli Studi di Pisa, Italy.